OPEN ACCESS

University of BRISTOL

Tayler, H. M., Palmer, J. C., Thomas, T. L., Kehoe, P. G., Paton, J. F. R., & Love, S. (2017). Cerebral A$_{40}$ and systemic hypertension. *Journal of Cerebral Blood Flow and Metabolism*. https://doi.org/10.1177/0271678X17724930

Peer reviewed version

Link to published version (if available):
10.1177/0271678X17724930

Link to publication record in Explore Bristol Research
PDF-document

University of Bristol - Explore Bristol Research
General rights

Cerebral Aβ$_{40}$ and systemic hypertension

Hannah M. Tayler[1]

Jennifer C. Palmer[1]

Taya L. Thomas[1]

Patrick G. Kehoe[1]

Julian F.R. Paton[2]

Seth Love[1]

[1] School of Clinical Sciences, University of Bristol, Bristol BS10 5NB, United Kingdom

[2] School of Physiology, Pharmacology & Neuroscience, Biomedical Sciences, University of Bristol, Bristol BS8 1TD, United Kingdom

Seth Love, University of Bristol, Level 2 Learning & Research, Southmead Hospital, Bristol, BS10 5NB. Telephone: +44 (0)117 41 42404. Email: seth.love@bristol.ac.uk

Running Title: Cerebral Aβ40 and systemic hypertension

1

Abstract

Mid-life hypertension and cerebral hypoperfusion may be preclinical abnormalities in people who later develop Alzheimer's disease (AD). Although accumulation of amyloid-beta (Aβ) is characteristic of AD and is associated with upregulation of the vasoconstrictor peptide endothelin-1 (EDN1) within the brain, it is unclear how this affects systemic arterial pressure. We have investigated whether infusion of $A\beta_{40}$ into ventricular cerebrospinal fluid (CSF) modulates blood pressure in the Dahl salt-sensitive rat. The Dahl salt-sensitive rat develops hypertension if given a high-salt diet. Intracerebroventricular infusion of Aβ induced a progressive rise in blood pressure (BP) in rats with pre-existing hypertension produced by a high-salt diet ($P < 0.0001$), but no change in BP in normotensive rats. The elevation in arterial pressure in high-salt rats was associated with an increase in low frequency spectral density in systolic blood pressure, suggesting autonomic imbalance, and reduced cardiac baroreflex gain. Our results demonstrate the potential for intracerebral Aβ to exacerbate hypertension, through modulation of autonomic activity. Present findings raise the possibility that mid-life hypertension in people who subsequently develop AD may in some cases be a physiological response to reduced cerebral perfusion complicating the accumulation of Aβ within the brain.

Key words: Alzheimer Disease; Amyloid-beta Peptides; Baroreflex; Dahl Salt-Sensitive Rats; Hypertension

Introduction

Hypertension affects at least one quarter of adults and more than half of those over 60 years.[1] It is a major risk factor for cognitive decline and vascular dementia (VaD)[2] and has been reported to increase the risk of developing Alzheimer's disease (AD)[3, 4] but the mechanisms are unclear. Cerebrovascular changes in AD include disruption to the blood-brain barrier (BBB), endothelial dysfunction, arterial stiffness and cerebral amyloid angiopathy (CAA).[5-7] Inadequate cerebral perfusion is an early-stage manifestation of AD and probably contributes to concomitant white matter pathology and cognitive decline.[8-13] Recent studies in humans implicate cerebrovascular hypotension as a driver of systemic hypertension as a mechanism to preserve cerebral blood flow.[14]

The identification of mid-life hypertension and cerebral hypoperfusion as preclinical abnormalities in people who later develop AD provides a potential opportunity for intervention to delay or slow disease. However, it remains unclear how the vascular and neurodegenerative processes interact. Studies in animal models suggest that hypertension and associated non-amyloid small vessel disease (SVD) may cause Aβ to accumulate within the brain.[15-17] Retrospective analysis showed Aβ plaque load to be higher in post-mortem brain tissue from AD patients with than without a history of hypertension,[18] supporting findings in animal models.

However, the converse possibility should also be considered: that mid-life metabolic and structural cerebrovascular alterations in people who subsequently develop AD, may induce hypertension.[14] In AD, intracerebral vascular tone, neurovascular coupling and autoregulation are disrupted by abnormalities that affect regulation of vascular calibre and reduce blood flow.[9] These abnormalities include cholinergic deafferentation of cortical blood vessels,[19] free radical-mediated cerebral vasoconstriction,[20-23] Aβ-mediated upregulation of endothelin-1 (EDN1) production,[8, 24-26] and an increase in brain angiotensin II mediated at least partly by a rise in the activity of angiotensin-converting enzyme (ACE).[27, 28] Maintenance of cerebral perfusion in the face of these metabolic abnormalities would require an increase in cerebral perfusion pressure, manifesting as systemic hypertension.[29-31]

Ageing is associated with progressive decline in cardiovascular autonomic reflexes, particularly baroreflex sensitivity.[32] The consequences can include increased BP variability, impaired responsiveness to challenges to BP, and an increased risk of sudden cardiac death. Altered baroreflex sensitivity is an

independent risk factor for the development of memory problems in older people.[33] There is evidence of autonomic dysfunction in most types of dementia. It is particularly common in Parkinson's disease dementia (PDD) and dementia with Lewy bodies (DLB), reflecting disruption to central autonomic pathways in the brain stem and hypothalamus. In AD, neurodegenerative changes affect autonomic nervous system pathways in the anterior cingulate, insular cortex and amygdala.[34] Patients with Lewy body diseases, AD and VaD have an increased prevalence of orthostatic hypotension.

Cardiovascular autonomic control mechanisms can be monitored by measurements of spontaneous fluctuations in heart rate and blood pressure, heart rate variability (HRV), systolic blood pressure variability (SBPV), and baroreflex gain (BRG) which provides information on the relative contribution of the baroreflex to control of heart rate. Impaired BRG may indicate cardiovascular or neurological disease. The baroreflex is essential for the short-term control of BP but may also influence BP over the longer term, although this is more controversial.[35]

Aβ, in particular Aβ_{40}, has been shown to induce vasoconstriction following topical application to isolated arteries[36] or direct administration to mouse cortex.[23] Application of Aβ_{40} but not Aβ_{42} to pial vessels impaired neurovascular coupling and reduced cerebral perfusion, replicating abnormalities of cerebral blood flow in a range of hAPP transgenic mouse models. Our aims in this study were to investigate whether intracerebroventricular (ICV) infusion of Aβ_{40} would induce hypertension, or augment hypertension in a hypertensive animal model. To manipulate these variables *in vivo*, we have used the Dahl salt-sensitive (DAHL/SS) rat in conjunction with intracerebroventricular (ICV) Aβ_{40} infusion. Aβ_{42} aggregates too readily for sustained delivery by infusion pump, whereas Aβ_{40} is more soluble, is the major species of Aβ in human cerebrospinal fluid (CSF) and, as noted above, is known to induce the constriction of pial vessels that we wanted to model by ICV infusion. Our hypotheses were that Aβ_{40} would exacerbate systemic hypertension, with more pronounced effects in the presence of pre-existing hypertension (high-salt DAHL/SS), and that the increase in blood pressure would be reflected in alterations in its neuro-humoral control.

Methods

Animals

4

All experimental procedures in this study were conducted in strict accordance with the UK Animals (Scientific Procedures) Act 1986 and approved by University of Bristol local ethical review committee. The study used male Dahl salt-sensitive 12-14-week old rats (from Charles River, UK) with a mean initial weight of 360 g (range 303-416 g – for details see Table 1). DAHL/SS rats develop hypertension when fed a high-salt diet (8% NaCl), whereas DAHL/SS rats fed a low-salt diet (0.3% NaCl) have blood pressure within the normal range (systolic BP < 140 mmHg).[37] DAHL/SS rats have other traits in common with many hypertensive humans, including insulin resistance, hyperlipidaemia with high serum cholesterol, and reduced renal function. Animals were fed a low-salt diet (0.3% NaCl) from weaning but half were subsequently preconditioned on a high-salt diet (8% NaCl) for 3 weeks prior to arrival. The two groups were fed these respective low- or high-salt diets throughout the study. Welfare assessments were conducted daily. The animals were housed at a constant 22°C under a 14:10 light/dark cycle with free access to food and water. Animals were initially accommodated in groups, before transfer to individual cages after implantation of the telemetry device. All data were analysed and are reported in accordance with ARRIVE guidelines.[38]

Study Design

Groups of 5 DAHL/SS rats were assigned to a low- or high-salt diet prior to arrival to our facility, according to a block randomization schedule determined by the supplier. Simple randomization was used to assign animals in each group to receive ICV infusion of saline or $A\beta_{40}$. The Aβ infusion model does not fully reproduce the complex neuropathology of AD but does allow for the precise study of Aβ-specific, time course-dependent changes.[39] A power calculation was performed to determine the minimum number (n = 6) of animals required for each experimental group; based on previous experience of similar studies, a conservative estimate of the standard deviation of mean blood pressure values ($\leq 10\%$) was used, giving 80% power to detect changes of 12% or more at the p = 0.05 level and 90% power to detect differences of 15% or more. Male DAHL/SS were 12-14 weeks of age prior to telemetry surgery (see below), Specific Pathogen Free (barrier-maintained) and experiment-naïve.

Experimental procedures

Telemetry device implantation:

A telemetry system (Data Sciences International, MN, US) was used to record arterial pressure. The telemetry device was implanted according to the method of Waki *et al.*[40] An aseptic laparotomy was performed under reversible general anaesthetic to expose the abdominal aorta. The catheter tip of a radio-telemetry device (PhysioTel® PA series transmitter model PA-C40) was implanted into the descending aorta and secured with tissue adhesive. The body of the device was placed in the abdominal cavity and secured to the abdominal wall during suture closure of the incision. After recovery from anaesthesia, rats were placed in individual cages on receiver platforms (PhysioTel® Receivers model RPC-1) connected to a CED1401 data acquisition interface and a computer running *Spike2* software (both Cambridge Electronic Design, UK), enabling continuous acquisition of data. Baseline telemetry data collection was started 5 d after telemetry surgery and continued for 5-7 d, prior to mini-osmotic pump surgery.

Mini-osmotic pump implantation:

10-12 d after implantation of the telemetry device, a mini-osmotic pump was inserted for ICV infusion of $A\beta_{40}$ or saline (control).[39, 41] Prior to surgery, the mini-osmotic pump and vinyl catheter (Alzet® osmotic pump model 2004 and Alzet® brain infusion kit 1; Charles River) were filled under aseptic conditions with a solution containing either $A\beta_{40}$ (1 mg/ml (231 μM) of stock solution prepared in 0.35% acetonitrile and diluted to the final concentration in sterile saline) or saline (with acetonitrile to the same final concentration). Under reversible general anaesthetic, the rat was placed in a stereotaxic frame and the skull exposed using aseptic surgical technique. The fine-gauge stainless steel cannula (brain infusion kit) was held in position by a clamp arm attached to the stereotaxic frame. The cannula was positioned and implanted below the skull surface into the right lateral ventricle (AP -1.0, L -1.6, D 5.0) and attached to the catheter and pump. The cannula was fixed in position and the mini-osmotic pump implanted subcutaneously. ICV osmotic infusion allowed continuous delivery of $A\beta_{40}$ or saline at 0.25 μl per hour over a 4-week period (equivalent to 0.006 mg of $A\beta_{40}$ per day). The rate of CSF production and removal in the rat is about 3.6 ml/d.[42] The physiological level of $A\beta_{40}$ in rat CSF is approximately 0.3-0.4 nM, so the addition of 0.006 mg/d $A\beta_{40}$ should elevate this by approximately 1000-fold to 385 nM. However, $A\beta_{40}$ is eliminated much more rapidly than the CSF itself,[43] so we estimate the mean level to have been raised by up to about 100-fold over the duration of the infusion.

Experimental Outcomes

6

Telemetry monitoring and data analysis:

Rats were fitted with a telemetry device capable of measuring arterial pulse pressure. Heart rate (HR), respiratory rate (RR), systolic (SBP), diastolic (DBP) and mean blood pressure (MBP) were derived from this waveform using *Spike2* software. The telemetry device was switched on 5 days after implantation to record for 5-7 days (baseline). Mean HR, RR, SBP, DBP and MBP were calculated for each 24-h period and an average baseline value for each parameter was determined. Following insertion of the ICV cannula, telemetry measurements were recorded at a digital sampling frequency of 100 Hz (low pass filter at 45 Hz) continuously from 3-28 days post-surgery and the average for each 24-h period was determined relative to mean baseline values.

HR and BP variability analysis

Spike2 software was used for spectral analysis of HR and SBP variability (HRV and SBPV). These indicators of autonomic function were analysed by separating the main peaks of the power spectrum in the frequency domain using a Fourier transform algorithm (Supplementary Figure 6). The three main components of the power spectrum were interpolated at specific frequencies: very low frequency (VLF) fluctuations at 0-0.26 Hz; low frequency (LF) fluctuations at 0.26-0.76 Hz; and high frequency (HF) fluctuations at 0.76-3.3 Hz. VLF, LF and HF measurements were made in absolute values of HR power (bpm^2/Hz) or SBP power (bpm^2/Hz).[40]

By use of *Spike2* software, an index of baroreceptor sensitivity was derived from spontaneous fluctuations and pulse interval, according the time-series method of Oosting *et al*:[44] (1) blood pressure and pulse interval traces are smoothed to minimize respiratory fluctuations; (2) episodes in which blood pressure rises or falls over several consecutive heartbeats (ramps) were identified; (3) ramp changes in blood pressure versus changes in pulse interval are plotted after delays of 3, 4 and 5 heartbeats; and (4) a linear best-fit of the relationship between changes in blood pressure and changes in pulse interval is calculated to estimate baroreceptor sensitivity, as described previously (Supplementary Figure 6).[40] A mean r^2 value > 0.7 for the three linear fits was used as a goodness-of-fit threshold, thereby excluding ramps with a poor straight-line fit. In younger adults with normal baroreflex function, no more than about 30% of spontaneous SBP ramps are compensated for by a progressive reflex change in pulse interval.[45]

7

This physiological behaviour is explained by the fact that the sinus node is not under the exclusive control of the baroreflex.

Tissue collection and preparation

Brain tissue and plasma samples were collected post mortem. Tissue homogenates were separately prepared from anterior, intermediate and posterior regions of each cerebral hemisphere, yielding 6 homogenates from each brain. Tissue was transferred to 2 mL screw-cap tubes with ceramic beads and 1% SDS homogenization buffer (1% SDS, 10 mM Tris base pH 6, 0.1 mM NaCl, 1 µM PMSF, 1 µg/ml Aprotinin) at 20% w/v. Tissue was homogenized for 2 x 20 s at 6000 rpm in a Precellys® homogenizer (Bertin Technologies, from Stretton Scientific, UK) and centrifuged at 13000 rpm for 15 min at 4°C. Homogenates were aliquoted and stored at -80°C. Blood samples were collected by cardiac puncture under terminal anaesthesia in EDTA tubes and centrifuged immediately at 6000 rpm for 5 min. The plasma supernatant was collected and stored in aliquots at -80°C. Total protein was quantified in tissue and plasma samples by Coomassie (Bradford) protein assay (Thermo Scientific, UK).

EDN1, Aβ$_{40}$ and ECE-2 sandwich ELISAs

EDN1 in plasma and brain homogenates was measured by sandwich ELISA using the Endothelin Pan Specific DuoSet ELISA kit (R&D Systems, UK). The recommended protocol was followed, with samples (diluted 1:4 in reagent diluent; 1% BSA in PBS, pH 7.2), standards (2-fold serial dilutions of EDN1 standard, 0.98-250 pg/ml) and blanks (reagent diluent alone) added to the plate for 2 h. Aβ$_{40}$ in plasma and brain homogenates was measured by sandwich ELISA, as described.[46, 47] Samples homogenates (total protein 0.05 mg/ml) or plasma (1:2 dilution), blanks and a 7-point standard curve of recombinant Aβ$_{40}$ (0.2 – 12.5 nM; Sigma-Aldrich, UK), prepared in PBS containing 1% 1,10 phenanthroline. ECE-2 was measured by sandwich ELISA, modified from Palmer *et al*.[24] Homogenate samples (1:2 dilution), blanks and seven serial dilutions of recombinant ECE-2 (R&D Systems) at 54.1 – 3460 ng/ml were added to wells in duplicate. For each assay, the bound antibody was detected with a 1:1 mixture of substrate solution (hydrogen peroxide and tetramethylbenzidine; R&D Systems) with 2N sulphuric acid to stop the reaction. The optical density was read at 450 nm (FLUOstar OPTIMA plate reader; BMG Labtech, Germany). To correct for any optical imperfections in the microplate, readings at 590 nm were subtracted from those at

450 nm. Sample concentrations of EDN1, $A\beta_{40}$ and ECE-2 were interpolated from the respective standard curve. Each sample was assayed in duplicate.

ECE-1 western blot

ECE-1 was measured by western blot with a biotinylated ECE-1 antibody (BAF1784, R&D systems), as described.[48] The antibody detects full-length ECE-1 at 120 kDa and a 75 kDa splice variant (ECE-1sv). Recombinant ECE-1 standard (1784ZN, R&D systems) was diluted to create a four-point standard curve (0.1 – 2.75 ng/µl) for each gel. Standards and samples of tissue homogenates (15 µg total protein) in SDS sample buffer were run on pre-cast gels before transfer to a nitrocellulose membrane. The primary antibody was added at 1:2000 in blocking buffer (3% BSA-TTBS) for 2 h. Streptavidin-conjugated peroxidase antibody was used for detection at 1:800 in blocking buffer. Each sample was measured in duplicate and the mean total ECE-1 + ECE-1sv concentration calculated.

ACE activity

ACE activity in brain homogenates and plasma was measured using the ACE1-specific fluorogenic substrate Abz-FRK(Dnp)-*P* (Biomol International) in the presence of the ACE-inhibitor, captopril (1 mM), as described by Miners *et al*.[27, 28] ACE capture antibody (MAB929), recombinant ACE standard (929-ZN, R&D Systems) and fluorogenic substrate (ES005) were all from R&D Systems. Fluorescence (320/405nm) was measured after overnight incubation. ACE activity measurements were interpolated from the standard curve using a 4-parameter curve fit.

Statistical Methods

Statistical analyses were performed in GraphPad Prism 6. All data sets were assessed for normality of distribution by the D'Agostino & Pearson test.

Baseline telemetry data (collected prior to mini-pump implantation) were log-transformed prior to analysis: the resultant parametric data were compared by unpaired samples *t*-test. Post-infusion telemetry data from each of the four sub-groups (low/high salt; Aβ/saline infusion) were compared by paired samples t-test to the respective baseline data. To compare the effects of Aβ and saline infusion, the telemetry data collected following infusion was adjusted relative to the corresponding sample pre-

9

infusion baseline mean and analysed for each 24-hour period; best-fit regression lines (for change in physiological parameter over time post-infusion) were compared by sum-of-squares *F*-test.

Biochemical data for each subgroup of animals were compared by *t*-test.

Results

Baseline Data

Mean baseline data are presented in Table 1. DAHL/SS rats fed the high-salt diet had significant (p < 0.0001) hypertension at baseline (MBP (mean ± SEM): 151 ± 6 mmHg) compared to those on the low-salt diet (MBP: 114 ± 2 mmHg).

Outcomes and Estimation

High salt DAHL/SS telemetry post-infusion

We compared the changes in HR, RR, MBP, SBP and DBP over baseline in Aβ- (n=6) and saline- (n=6) infused high-salt DAHL/SS rats from 3-28 d post-infusion (Supplementary Figure 1). BP increased over time in both saline- and Aβ-infused rats but the increase was markedly greater in the Aβ-infused animals. Comparison of best-fit regression lines by sum-of-squares *F*-test showed that the increases in MBP, SBP and DBP were much greater in Aβ-infused than saline-infused animals, and the decline in HR and RR less marked (p < 0.0001 for all five comparisons; Figure 1). The BP increase in the saline-infused group was accompanied by a drop in both HR and RR over time. The HR and RR of the Aβ-infused group did not change over the infusion period, despite the greater BP increase. In the final week following infusion (days 22-28 inclusive), MBP relative to pre-infusion baseline had increased by 21 ± 11 mmHg (mean ± SD) in the Aβ group (t (5) = 4.73, p = 0.005), compared to 11 ± 8 mmHg in the saline group (t (5) = 3.64, p = 0.015; Supplementary Figure 4 (A)).

Low-salt DAHL/SS telemetry post-infusion

We compared the changes in HR, RR, MBP, SBP and DBP with respect to baseline mean in Aβ- (n=8) and saline- (n=7) infused low-salt DAHL/SS rats (Supplementary Figure 2). Comparison of best-fit regression lines by sum-of-squares *F*-test revealed no differences in MBP, SBP or DBP between the Aβ- and saline-

10

infused groups. Small but significant reductions were found in both HR and RR (P < 0.0001 for both) in the Aβ- compared to the saline-infused animals (Figure 2). MBP was marginally elevated by 3 ± 3 mmHg following Aβ infusion (days 22-28 mean vs. baseline mean; t (5) = 2.95, p = 0.022), but did not differ significantly after saline infusion (Supplementary Figure 4 (B)). This finding should be interpreted with caution as there was not a significant difference between Aβ- and saline-infusion by regression line comparison and the possibility of a type I statistical error cannot be excluded.

Heart rate variability, systolic blood pressure variability and baroreflex gain in high-salt DAHL/SS post-infusion

Data available for a subset of high-salt DAHL/SS (Aβ: n = 5; saline: n = 3) from 3-21 d post-infusion were analysed for HRV, SBPV and BRG (Supplementary Figure 3). A sum-of squares F-test comparison tested the null hypothesis (H_0) that a single linear regression line could fit the combined data sets. We found no significant difference in the VLF ($F_{2,148}$ = 0.120, ns) or LF component ($F_{2,148}$ = 2.507, ns) of HRV (change in bpm^2/Hz) between the saline- and Aβ-infused rats (H_0 accepted; Figure 3 (A-B)). The HF component of HRV, reflecting respiration, increased over time in the saline group but remained at baseline in the Aβ$_{40}$-infusion group ($F_{2,148}$ = 10.64, p < 0.0001; H_0 rejected; Figure 3 (C)). A comparison of best-fit lines for the VLF, LF and HF components (mmHg^2/Hz) of SBPV demonstrated that each increased significantly in the Aβ- compared to the saline-infusion group (VLF $F_{2,148}$ = 17.46, LF: $F_{2,148}$ = 15.59 both p<0.0001; HF: $F_{2,148}$ = 17.46 p<0.0005; H_0 rejected; Figure 3 (D-F)).

We compared the relative change in BRG over baseline in a subset of Aβ- (n = 5) and saline-infused (n = 3) high-salt DAHL/SS rats from 3-28 d post-infusion. There was a progressive decline in both positive ($F_{2,202}$ = 28.91, p < 0.0001) and negative ramps ($F_{2,202}$ = 4.761, p < 0.001) over the 28 days following Aβ$_{40}$ infusion but little change after saline infusion (H_0 rejected; Figure 3 (G-H)). Comparison of best-fit regression lines showed that the data from the Aβ- and saline-infused groups differed significantly for both positive (p < 0.0001) and negative (p < 0.01) ramps, indicating a reduction in the sensitivity of the baroreflex response over time during Aβ infusion.

Aβ$_{40}$ level in brain tissue homogenates and plasma

The level of Aβ$_{40}$ (measured by sandwich ELISA) remaining in the brain after completion of the infusions was measured in homogenates of anterior, medial and posterior thirds of the left and right hemispheres.

11

We found no consistent differences between groups, either when comparing individual brain regions or when the measurements were combined to indicate the mean for each case (Supplementary Figure 5 (A)). $A\beta_{40}$ is cleared quite rapidly from the CSF[43, 49] and although there is some penetration of the brain parenchyma[39] it does not aggregate to any significant extent.[50] The finding that $A\beta_{40}$ was not significantly elevated in the brain tissue of the rats that had received ICV infusion of $A\beta$ is in keeping with these previous studies and suggests that infused $A\beta$ peptide which may have penetrated the brain had been largely cleared from the brain by the time that the tissue was collected, i.e. after completion of the 4-weeks of infusion.

We also measured $A\beta_{40}$ in plasma samples. The levels of peptide for several cases fell below the detection limit of the sandwich ELISA. No significant differences were found between the $A\beta$-infused groups in either the high salt or low salt DAHL/SS (Supplementary Figure 5 (B)).

EDN1, ECE-1, ECE-2 and ACE activity

We did not find significant differences between $A\beta$- and saline-infused rats in the level of EDN1, ECE-1, ECE-2 or ACE activity in brain homogenates, when either the mean values for the whole brain (Supplementary Figure 5 (C-F)) or the values for anterior, intermediate and posterior regions of each cerebral hemisphere (data not shown) were compared between subgroups. We also found no significant difference in ACE activity in plasma between $A\beta$- and saline-infused groups (Supplementary Figure 5 (G)).

Adverse Events

One animal from the high salt/$A\beta_{40}$ infused group experienced a late failure of the aortic telemetry implant, 3 weeks after infusion surgery.

Discussion

In this study, we investigated the physiological effects of ICV $A\beta_{40}$ peptide in a rat model of conditional hypertension (dependent on dietary salt intake). $A\beta$ ICV infusion induced a progressive, highly significantly rise in BP in rats with pre-existing hypertension (high salt DAHL/SS) but no change in BP in rats that were normotensive (low salt DAHL/SS) prior to infusion. Our results suggest that $A\beta$ has the potential to increase BP, particularly in the context of pre-existing hypertension.

The hypertension induced by Aβ may be a protective response to cerebral hypoperfusion. In a series of 259 normotensive and hypertensive adults, Warnert et al.[14] found that hypertension was associated with vertebral artery hypoplasia, an incomplete posterior circle of Willis, increased cerebral vascular resistance and reduced cerebral blood flow. There is a substantial literature suggesting that Aβ increases cerebral vascular resistance and reduces cerebral blood flow. Topical application of $Aβ_{40}$ to isolated arteries or to mouse cortex in vivo was shown to induce vasoconstriction.[23, 36] In mice overexpressing mutant amyloid-β precursor protein (Tg2576), excess endogenous Aβ was shown to induce vasoconstriction and inhibit autoregulation and neurovascular coupling.[20, 21, 23] Our results demonstrate the prolonged effects of long-term infusion with $Aβ_{40}$ on BP, and differ somewhat from previous *in vivo* studies which had a short infusion period. For example, Sprague-Dawley rats given short-term intra-arterial infusion of $Aβ_{40}$ showed a substantial increase of MBP but only in hypotensive animals, with no change in normotensive animals. In the same study, vehicle infusion in spontaneously hypertensive animals induced a significant reduction in BP which was abolished by the infusion of $Aβ_{40}$.[51] In another study, mice were given subcutaneous DOCA-salt implants to induce hypertension, followed by subcutaneous $Aβ_{40}$ over 30-45 minutes; the increase in MBP was no different between animals that received $Aβ_{40}$ and those given vehicle, but the former showed an attenuated response to ACh.[52]

Aβ has multiple cerebrovascular effects that influence the regulation of CBF (for review see[7, 9]). Cerebral perfusion declines several years before the development of dementia, in both sporadic[11] and familial AD,[10] particularly in brain regions with early accumulation of Aβ,[10] and this is associated with preclinical white matter damage (i.e. the fall in perfusion exceeds the decline in metabolic demand and causes tissue injury).[12] Further evidence of a deficit in cerebral perfusion in AD comes from studies showing elevation of vascular endothelial growth factor, and significantly greater loss of the ischaemia-sensitive myelin-associated glycoprotein (MAG) than the relatively resistant proteolipid protein-1 (PLP-1).[7-9, 53-55] Hypoxic alterations in brain tissue in early AD correlate closely with Aβ accumulation.[9] Aβ accumulation also correlates with BBB leakage, indicating involvement of multiple components of the neurovascular unit in AD.[56] There is a complex relationship between Aβ, BBB dysfunction and cerebral hypoperfusion, whereby BBB dysfunction reduces blood flow and impairs Aβ clearance,[57, 58] and Aβ damages the BBB through pericytic[57, 59, 60] and endothelial toxicity and increased monocyte adhesion.[61] A

13

sustained reduction in cerebral blood flow might be expected to induce systemic hypertension, as a homeostatic response to restore blood flow by raising perfusion pressure. [29-31]

Aβ infusion had sustained or progressive effects on multiple cardiovascular control mechanisms, as evidenced by the changes in heart rate and blood pressure variability, and in baroreflex responsiveness. These physiological alterations were most marked in the hypertensive (high-salt) animals and included elevation of VLF, LF and HF components of SBPV but not significant alterations in HRV. The interpretation of and physiological basis for SBPV are somewhat contentious, but there is agreement that the LF and VLF components involve sympathetic supply to arteries.[62] The physiological data suggest strongly that elevated sympathetic activity contributed to the increase in total peripheral resistance underling the hypertensive effects of Aβ.

Both HRV and SBPV are altered in AD, with some changes evident before development of dementia. For example, patients with mild AD and MCI have altered HRV and SBPV in response to orthostatic stress.[63] Lower cognitive performance was associated with altered HRV in AD, evidence of elevated cardiac sympathetic activity (LF:HF power ratio) and lower parasympathetic activity (HF power).[64] Increased SBPV variability (adjusted for raised SBP average itself and monitored over medium to long periods) is associated more generally with negative clinical outcomes, cardiovascular events, mortality and stroke.[65] In a study of 25,000 people at high risk of cardiovascular disease, the risk of developing cognitive impairment was elevated in patients with greater variability of visit-to-visit BP, independent of the absolute BP itself.[66]

Aβ infusion affected control of the baroreceptor reflex. This is also compromised in AD. Compared to age-matched control, AD patients had depressed baroreflex sensitivity.[67] In a further study, baroreflex values were lower in AD than in controls or MCI, and differed significantly between MCI and controls.[68] These changes presumably reflect alterations (functional or structural) to brain regions involved in the baroreflex regulation of sympathetic activity, for example adrenaline-synthesizing medullary neurons (around 30% of which are lost in AD) and noradrenergic neurons in the locus coeruleus, affected by neurofibrillary tangles and neurodegeneration in early AD.[64, 69] Baroreflex sensitivity in midlife has a positive association with regional perfusion to the hippocampus (hypoperfused in apparently healthy, middle-aged normotensive adults in whom baroreflex sensitivity is reduced).[70] In older adults (65 ± 6 y)

with and without MCI, stiffness of central arteries and depressed baroreflex sensitivity correlated independently with white matter lesions.[71]

Alterations to the activity of the sympathetic nervous system and baroreflex could be driving the hypertension observed in this study. Central administration of $A\beta_{40}$ to the lateral ventricle may mediate the raised sympathetic activity and reduced BRG via NADPH oxidase-mediated production of reactive oxygen species (ROS) and/or downregulation of nitric oxide synthase (NOS). Oxidative stress plays a role in the generation and maintenance of arterial hypertension in human and several animal models, including the DAHL/SS rat. Oxidative stress in the brain is linked to hypertension pathogenesis via reductions to baroreflex sensitivity and activation of the sympathetic nervous system.[72] The hypertensive effects of high-salt in DAHL/SS rats are partly mediated by increased activity of NADPH oxidase and the production of higher levels of ROS, and impaired vasodilation resulting from reduced activity of NOS. NADPH-derived ROS and associated reduction in bioavailability of nitric oxide probably contribute to the cerebrovascular dysfunction induced by $A\beta$.[73]

We investigated two potential mechanisms whereby $A\beta$ might have increased cerebral vascular resistance and induced hypertension: upregulation of EDN1 production and elevation of ACE activity. We did not find evidence of significant changes in either pathway but it is difficult to interpret these end-stage analyses, as they were conducted after depletion of the $A\beta$ infusate; according to the manufacturer, the delivery of infusate by the osmotic pumps is constant for approximately 28 d but then declines rapidly, and in keeping with this we found little residual $A\beta_{40}$ in brain tissue homogenates after this period. It seems most likely that the peptide is cleared relatively quickly in this model. Rapid turnover of $A\beta_{40}$ was previously demonstrated in APP transgenic mice, with a half-life of approximately 0.7 h for soluble, non-deposited forms of $A\beta_{40}$.[74] Limitations of the present study include the relatively small sample sizes for the measurements of some of the baroreflex and variability data, and our use of supra-physiological levels of $A\beta_{40}$ to model the effects of chronic $A\beta$-induced cerebral hypoperfusion but over a much shorter period than would apply in human Alzheimer's disease. In addition, we did not assess hypoperfusion by measurement of vascular endothelial growth factor or the MAG:PLP-1 ratio in this series of experiments but that would certainly be of interest in future studies.

In conclusion, we have shown that ICV infusion of $A\beta_{40}$ over a 4-week period alters autonomic control of cardiovascular function, causing progressive elevation in systemic blood pressure in rats with

15

pre-existing hypertension. These findings raise the possibility that (i) mid-life hypertension may, in some cases, be a physiological response to reduced cerebral perfusion complicating the accumulation of Aβ within the brain, and (ii) cerebral accumulation of Aβ may be particularly likely to exacerbate pre-existing hypertension.

Authors' contributions

All experiments were performed at the University of Bristol. The study was conceived by SL, and designed by SL, JCP and PK. JCP designed and optimized the surgical procedures. HMT and JCP executed and analysed the *in vivo* studies. HMT and TLT performed the telemetry analyses and biochemical experiments. HMT wrote the manuscript with feedback from JCP, SL, PGK and JFRP.

Competing interests

The authors have no competing interests to disclose with respect to the research, authorship, and/or publication of this article.

Supplementary material

Supplementary material for this paper can be found at

http://jcbfm.sagepub.com/content/by/supplemental-data.

References

1.   Kearney PM, Whelton M, Reynolds K, et al. Global burden of hypertension: analysis of worldwide data. *Lancet*. 2005; 365: 217-223.

2.   Tzourio C. Hypertension, cognitive decline, and dementia: an epidemiological perspective. *Dialogues Clin Neurosci*. 2007; 9: 61-70.

3.   Power MC, Weuve J, Gagne JJ, et al. The association between blood pressure and incident Alzheimer disease: a systematic review and meta-analysis. *Epidemiology*. 2011; 22: 646-659.

4.   Gottesman RF, Schneider AL, Albert M, et al. Midlife hypertension and 20-year cognitive change: the atherosclerosis risk in communities neurocognitive study. *JAMA Neurol*. 2014; 71: 1218-1227.

5.   Attems J and Jellinger KA. The overlap between vascular disease and Alzheimer's disease–lessons from pathology. *BMC Med*. 2014; 12: 206.

6.   Kalaria RN and Ballard C. Overlap between pathology of Alzheimer disease and vascular dementia. *Alzheimer Dis Assoc Disord*. 1999; 13 Suppl 3: S115-123.

7.   Love S and Miners JS. Cerebrovascular disease in ageing and Alzheimer's disease. *Acta Neuropathol*. 2016; 131: 645-658.

8.   Miners JS, Palmer J and Love S. Pathophysiology of hypoperfusion of the precuneus in early Alzheimer's disease. *Brain Pathol*. 2016; 26: 533-541.

9.   Miners JS and Love S. Cerebral hypoperfusion and the energy deficit in Alzheimer's disease. *Brain Pathol*. 2016; 26: 607-617.

10.   Benzinger TL, Blazey T, Jack CR, Jr., et al. Regional variability of imaging biomarkers in autosomal dominant Alzheimer's disease. *Proc Natl Acad Sci U S A*. 2013; 110: E4502-4509.

11.   Binnewijzend MA, Kuijer JP, Benedictus MR, et al. Cerebral blood flow measured with 3D pseudocontinuous arterial spin-labeling MR imaging in Alzheimer disease and mild cognitive impairment: a marker for disease severity. *Radiology*. 2013; 267: 221-230.

12.   Lee S, Viqar F, Zimmerman ME, et al. White matter hyperintensities are a core feature of Alzheimer's disease: Evidence from the dominantly inherited Alzheimer network. *Ann Neurol*. 2016; 79: 929-939.

13.   Tarumi T, Dunsky DI, Khan MA, et al. Dynamic cerebral autoregulation and tissue oxygenation in amnestic mild cognitive impairment. *J Alzheimers Dis*. 2014; 41: 765-778.

14.   Warnert EA, Rodrigues JC, Burchell AE, et al. Is high blood pressure self-protection for the brain? *Circ Res*. 2016; 119: e140-e151.

15.   Bueche CZ, Hawkes C, Garz C, et al. Hypertension drives parenchymal β-amyloid accumulation in the brain parenchyma. *Ann Clin Transl Neurol*. 2014; 1: 124-129.

16.   Carnevale D, Mascio G, Ajmone-Cat MA, et al. Role of neuroinflammation in hypertension-induced brain amyloid pathology. *Neurobiol Aging*. 2012; 33: 205.e219-205.e229.

17.   Carnevale D, Mascio G, D'Andrea I, et al. Hypertension induces brain β-amyloid accumulation, cognitive impairment, and memory deterioration through activation of receptor for advanced glycation end products in brain vasculature. *Hypertension*. 2012; 60: 188-197.

18.   Ashby EL, Miners JS, Kehoe PG, et al. Effects of hypertension and anti-hypertensive treatment on amyloid-β (Aβ) plaque load and Aβ-synthesizing and Aβ-degrading enzymes in frontal cortex. *J Alzheimers Dis*. 2016; 50: 1191-1203.

17

19.   Tong XK and Hamel E. Regional cholinergic denervation of cortical microvessels and nitric oxide synthase-containing neurons in Alzheimer's disease. *Neuroscience*. 1999; 92: 163-175.

20.   Niwa K, Carlson GA and Iadecola C. Exogenous Aβ1-40 reproduces cerebrovascular alterations resulting from amyloid precursor protein overexpression in mice. *J Cereb Blood Flow Metab*. 2000; 20: 1659-1668.

21.   Niwa K, Kazama K, Younkin SG, et al. Alterations in cerebral blood flow and glucose utilization in mice overexpressing the amyloid precursor protein. *Neurobiol Dis*. 2002; 9: 61-68.

22.   Niwa K, Porter VA, Kazama K, et al. Aβ-peptides enhance vasoconstriction in cerebral circulation. *Am J Physiol Heart Circ Physiol*. 2001; 281: H2417-2424.

23.   Niwa K, Younkin L, Ebeling C, et al. Aβ1-40-related reduction in functional hyperemia in mouse neocortex during somatosensory activation. *Proc Natl Acad Sci U S A*. 2000; 97: 9735-9740.

24.   Palmer JC, Baig S, Kehoe PG, et al. Endothelin-converting enzyme-2 is increased in Alzheimer's disease and up-regulated by Aβ. *Am J Pathol*. 2009; 175: 262-270.

25.   Palmer JC, Barker R, Kehoe PG, et al. Endothelin-1 is elevated in Alzheimer's disease and upregulated by amyloid-β. *J Alzheimers Dis*. 2012; 29: 853-861.

26.   Palmer JC, Tayler HM and Love S. Endothelin-converting enzyme-1 activity, endothelin-1 production, and free radical-dependent vasoconstriction in Alzheimer's disease. *J Alzheimers Dis*. 2013; 36: 577-587.

27.   Miners JS, Ashby E, Van Helmond Z, et al. Angiotensin-converting enzyme (ACE) levels and activity in Alzheimer's disease, and relationship of perivascular ACE-1 to cerebral amyloid angiopathy. *Neuropathol Appl Neurobiol*. 2008; 34: 181-193.

28.   Miners S, Ashby E, Baig S, et al. Angiotensin-converting enzyme levels and activity in Alzheimer's disease: differences in brain and CSF ACE and association with ACE1 genotypes. *Am J Transl Res*. 2009; 1: 163-177.

29.   Warnert EA, Rodrigues JC, Burchell AE, et al. Is High Blood Pressure Self-Protection for the Brain? *Circ Res*. 2016.

30.   Cates MJ, Steed PW, Abdala AP, et al. Elevated vertebrobasilar artery resistance in neonatal spontaneously hypertensive rats. *J Appl Physiol*. 2011; 111: 149-156.

31.   Paton JF, Dickinson CJ and Mitchell G. Harvey Cushing and the regulation of blood pressure in giraffe, rat and man: introducing 'Cushing's mechanism'. *Exp Physiol*. 2009; 94: 11-17.

32.   Monahan KD. Effect of aging on baroreflex function in humans. *Am J Physiol Regul Integr Comp Physiol*. 2007; 293: R3-R12.

33.   Saint Martin M, Sforza E, Thomas-Anterion C, et al. Baroreflex sensitivity, vascular risk factors, and cognitive function in a healthy elderly population: the PROOF cohort. *J Am Geriatr Soc*. 2013; 61: 2096-2102.

34.   Idiaquez J and Roman GC. Autonomic dysfunction in neurodegenerative dementias. *J Neurol Sci*. 2011; 305: 22-27.

35.   La Rovere MT, Pinna GD and Raczak G. Baroreflex sensitivity: measurement and clinical implications. *Ann Noninvasive Electrocardiol*. 2008; 13: 191-207.

36.   Crawford F, Suo Z, Fang C, et al. Characteristics of the *in vitro* vasoactivity of β-amyloid peptides. *Exp Neurol*. 1998; 150: 159-168.

37.   Rapp JP. Dahl salt-susceptible and salt-resistant rats. A review. *Hypertension*. 1982; 4: 753-763.

38.   McGrath JC, Drummond GB, McLachlan EM, et al. Guidelines for reporting experiments involving animals: the ARRIVE guidelines. *Br J Pharmacol*. 2010; 160: 1573-1576.

39.   Nitta A, Itoh A, Hasegawa T, et al. β-Amyloid protein-induced Alzheimer's disease animal model. *Neurosci Lett*. 1994; 170: 63-66.

40.   Waki H, Kasparov S, Katahira K, et al. Dynamic exercise attenuates spontaneous baroreceptor reflex sensitivity in conscious rats. *Exp Physiol*. 2003; 88: 517-526.

41.   Srivareerat M, Tran TT, Alzoubi KH, et al. Chronic psychosocial stress exacerbates impairment of cognition and long-term potentiation in β-amyloid rat model of Alzheimer's disease. *Biol Psychiatry*. 2009; 65: 918-926.

42.   Chiu C, Miller MC, Caralopoulos IN, et al. Temporal course of cerebrospinal fluid dynamics and amyloid accumulation in the aging rat brain from three to thirty months. *Fluids Barriers CNS*. 2012; 9: 3-3.

43.   Fujiyoshi M, Tachikawa M, Ohtsuki S, et al. Amyloid-beta peptide(1-40) elimination from cerebrospinal fluid involves low-density lipoprotein receptor-related protein 1 at the blood-cerebrospinal fluid barrier. *J Neurochem*. 2011; 118: 407-415.

44.   Oosting J, Struijker-Boudier HA and Janssen BJ. Validation of a continuous baroreceptor reflex sensitivity index calculated from spontaneous fluctuations of blood pressure and pulse interval in rats. *J Hypertens*. 1997; 15: 391-399.

45.   Di Rienzo M, Parati G, Castiglioni P, et al. Baroreflex effectiveness index: an additional measure of baroreflex control of heart rate in daily life. *Am J Physiol Regul Integr Comp Physiol*. 2001; 280: R744-751.

46.   Van Helmond Z, Miners JS, Kehoe PG, et al. Higher soluble amyloid β concentration in frontal cortex of young adults than in normal elderly or Alzheimer's disease. *Brain Pathol*. 2010; 20: 787-793.

47.   Miners JS, Jones R and Love S. Differential changes in Aβ42 and Aβ40 with age. *J Alzheimers Dis*. 2014; 40: 727-735.

48.   Palmer JC, Kehoe PG and Love S. Endothelin-converting enzyme-1 in Alzheimer's disease and vascular dementia. *Neuropathol Appl Neurobiol*. 2010; 36: 487-497.

49.   Bateman RJ, Munsell LY, Morris JC, et al. Human amyloid-β synthesis and clearance rates as measured in cerebrospinal fluid in vivo. *Nat Med*. 2006; 12: 856-861.

50.   Frautschy SA, Yang F, Calderon L, et al. Rodent models of Alzheimer's disease: rat Aβ infusion approaches to amyloid deposits. *Neurobiol Aging*. 1996; 17: 311-321.

51.   Arendash GW, Su GC, Crawford FC, et al. Intravascular β-amyloid infusion increases blood pressure: implications for a vasoactive role of beta-amyloid in the pathogenesis of Alzheimer's disease. *Neurosci Lett*. 1999; 268: 17-20.

52.   Faraco G, Park L, Zhou P, et al. Hypertension enhances Aβ-induced neurovascular dysfunction, promotes β-secretase activity, and leads to amyloidogenic processing of APP. *J Cereb Blood Flow Metab*. 2016; 36: 241-252.

53.   Barker R, Ashby EL, Wellington D, et al. Pathophysiology of white matter perfusion in Alzheimer's disease and vascular dementia. *Brain*. 2014; 137: 1524-1532.

54.   Barker R, Wellington D, Esiri MM, et al. Assessing white matter ischemic damage in dementia patients by measurement of myelin proteins. *J Cereb Blood Flow Metab*. 2013; 33: 1050-1057.

55.   Thomas T, Miners S and Love S. Post-mortem assessment of hypoperfusion of cerebral cortex in Alzheimer's disease and vascular dementia. *Brain*. 2015; 138: 1059-1069.

56.   van de Haar HJ, Jansen JF, van Osch MJ, et al. Neurovascular unit impairment in early Alzheimer's disease measured with magnetic resonance imaging. *Neurobiol Aging*. 2016; 45: 190-196.

57.   Sagare AP, Bell RD, Zhao Z, et al. Pericyte loss influences Alzheimer-like neurodegeneration in mice. *Nat Commun*. 2013; 4: 2932.

58.   Sagare AP, Bell RD and Zlokovic BV. Neurovascular defects and faulty amyloid-β vascular clearance in Alzheimer's disease. *J Alzheimers Dis*. 2013; 33 Suppl 1: S87-100.

59.   Sagare AP, Sweeney MD, Makshanoff J, et al. Shedding of soluble platelet-derived growth factor receptor-β from human brain pericytes. *Neurosci Lett*. 2015; 607: 97-101.

60.   Verbeek MM, Van Nostrand WE, Otte-Holler I, et al. Amyloid-β-induced degeneration of human brain pericytes is dependent on the apolipoprotein E genotype. *Ann N Y Acad Sci*. 2000; 903: 187-199.

61.   Burgmans S, van de Haar HJ, Verhey FR, et al. Amyloid-β interacts with blood-brain barrier function in dementia: a systematic review. *J Alzheimers Dis*. 2013; 35: 859-873.

62.   Malpas SC. Neural influences on cardiovascular variability: possibilities and pitfalls. *Am J Physiol Heart Circ Physiol*. 2002; 282: H6-20.

20

63.   Mellingsæter MR, Wyller TB, Ranhoff AH, et al. Reduced sympathetic response to head-up tilt in subjects with mild cognitive impairment or mild Alzheimer's dementia. *Dement Geriatr Cogn Dis Extra*. 2015; 5: 107-115.

64.   Nonogaki Z, Umegaki H, Makino T, et al. Relationship between cardiac autonomic function and cognitive function in Alzheimer's disease. *Geriatr Gerontol Int*. 2015; 17: 92-98.

65.   Stevens SL, Wood S, Koshiaris C, et al. Blood pressure variability and cardiovascular disease: systematic review and meta-analysis. *BMJ*. 2016; 354: i4098.

66.   Böhm M, Schumacher H, Leong D, et al. Systolic blood pressure variation and mean heart rate is associated with cognitive dysfunction in patients with high cardiovascular risk. *Hypertension*. 2015; 65: 651-661.

67.   Szili-Török T, Kálmán J, Paprika D, et al. Depressed baroreflex sensitivity in patients with Alzheimer's and Parkinson's disease. *Neurobiol Aging*. 2001; 22: 435-438.

68.   den Abeelen AS, Lagro J, van Beek AH, et al. Impaired cerebral autoregulation and vasomotor reactivity in sporadic Alzheimer's disease. *Curr Alzheimer Res*. 2014; 11: 11-17.

69.   Braak H and Braak E. Neuropathological stageing of Alzheimer-related changes. *Acta Neuropathol*. 1991; 82: 239-259.

70.   Laosiripisan J, Tarumi T, Gonzales MM, et al. Association between cardiovagal baroreflex sensitivity and baseline cerebral perfusion of the hippocampus. *Clin Auton Res*. 2015; 25: 213-218.

71.   Tarumi T, de Jong DL, Zhu DC, et al. Central artery stiffness, baroreflex sensitivity, and brain white matter neuronal fiber integrity in older adults. *Neuroimage*. 2015; 110: 162-170.

72.   Peterson JR, Sharma RV and Davisson RL. Reactive oxygen species in the neuropathogenesis of hypertension. *Curr Hypertens Rep*. 2006; 8: 232-241.

73.   Park L, Anrather J, Zhou P, et al. NADPH-oxidase-derived reactive oxygen species mediate the cerebrovascular dysfunction induced by the amyloid β peptide. *J Neurosci*. 2005; 25: 1769-1777.

74.   Abramowski D, Wiederhold K-H, Furrer U, et al. Dynamics of Aβ turnover and deposition in different β-amyloid precursor protein transgenic mouse models following γ-secretase inhibition. *J Pharmacol Exp Ther*. 2008; 327: 411-424.

Table 1 Pre-infusion baseline telemetry data

Group	N	Weight* (g)	MBP (mmHg)	SBP (mmHg)	DBP (mmHg)	HR (bpm)	RR (breaths/min)
High Salt	12	361 ± 6	151 ± 6 [1]	169 ± 7 [1]	134 ± 5 [1]	373 ± 5	92 ± 4 [2]
Low Salt	15	359 ± 9	114 ± 2	127 ± 2	103 ± 2	364 ± 4	82 ± 3

Pre-infusion baseline telemetry data in high- and low-salt groups. Mean values ± SEM. *Weight prior to telemetry surgery at 12-14 weeks of age. Baseline MBP, SBP, DBP and RR were significantly higher in the high- than the low-salt group ([1] = $p < 0.0001$, [2] = $p < 0.05$). (Key: MBP, SBP, DBP = mean, systolic and diastolic blood pressure; HR =heart rate; RR = respiratory rate).

Legends to Figures

Figure 1 Change in BP, HR and RR in High-Salt DAHL/SS

Change in BP, HR and RR in high salt DAHL/SS over 28 d of Aβ (n=6) or saline (n=6) infusion. Each data point represents the group mean value on a given day during infusion. Best-fit linear regression (solid) and 95% CI (dotted) lines are shown. A comparison (sum-of-squares F-test) of best-fit regression lines tested the null hypothesis (H_0) that a single linear regression line could fit the combined data sets for the change in HR, RR, MBP, SBP and DBP, relative to baseline, after infusion of Aβ or saline. H_0 was rejected for each comparison. There was a highly significant greater effect of Aβ infusion compared to control (saline) infusion on (A) MBP ($F_{2,288}$ = 38.45, p < 0.0001), (B) SBP ($F_{2,288}$ = 61.50, p < 0.0001), (C) DBP ($F_{2,288}$ = 19.95, p < 0.0001), (D) HR ($F_{2,288}$ = 23.94, p < 0.0001), (E) RR ($F_{2,288}$ = 26.51, p < 0.0001). The increase in MBP, SBP and DBP was much greater in $Aβ_{40}$- than saline-infused animals (P < 0.0001), and the decline in HR and RR less marked (P < 0.0001).

Figure 2 Change in BP, HR and RR in Low-Salt DAHL/SS

Change in (A) MBP, (B) SBP, (C) DBP, (D) HR and (E) RR in Aβ- (n=8) or saline-infused (n=7) DAHL/SS rats on low salt diet. A sum-of squares F-test comparison tested the null hypothesis (H_0) that a single linear regression line could fit the combined data sets. H_0 was accepted for MBP, SBP and DBP but rejected for HR and RR. There was no significant effect of Aβ infusion compared to control (saline) infusion on either MBP ($F_{2,328}$ = 1.138, p > 0.05), SBP ($F_{2,328}$ = 2.386, p > 0.05) or DBP ($F_{2,328}$ = 0.632, ns). As the best-fit lines for blood pressure (MBP, SBP and DBP) did not differ significantly, a shared best-fit line is shown for the two infusion groups. There was a significant effect of Aβ infusion compared to control (saline) on both HR ($F_{2,328}$ = 19.24, p < 0.0001) and RR ($F_{2,325}$ = 11.59, p < 0.0001). Individual best-fit lines are shown for HR and RR.

Figure 3 Change in HRV, SBPV and BRG in High-Salt DAHL/SS

Change in HRV, SBPV and mean BRG in high salt DAHL/SS after Aβ (n=5) or saline (n=3) infusion. There were no significant effects of Aβ infusion on the (A) VLF ($F_{2,148}$ = 0.120, ns) and (B) LF ($F_{2,148}$ = 2.507, ns) components of HRV. There was a significant effect of Aβ infusion on (C) HF ($F_{2,148}$ = 10.64, p < 0.0001). There was a significant effect of Aβ infusion on (D) VLF ($F_{2,148}$ = 17.46, p < 0.0001), (E) LF ($F_{2,148}$ = 15.59, p

23

< 0.0001), and (F) HF ($F_{2,148}$ = 17.46, p < 0.0005) components of SBPV. There was a significant difference in the change in mean BRG (Mn.BRG) (G) positive ($F_{2,202}$ = 28.91, p < 0.0001) and (H) negative ($F_{2,202}$ = 4.761, p < 0.001) ramps during Aβ compared with saline infusion. Data are presented as daily group means, with lines of best-fit (solid) and 95% CI (dotted). A combined best-fit line is shown for both infusion groups when the H$_0$ was accepted (A-B). Separate lines for Aβ- and saline- infusion groups are shown when the H$_0$ was rejected (C-H).

Figures

Figure 4 Change in BP, HR and RR in High-Salt DAHL/SS
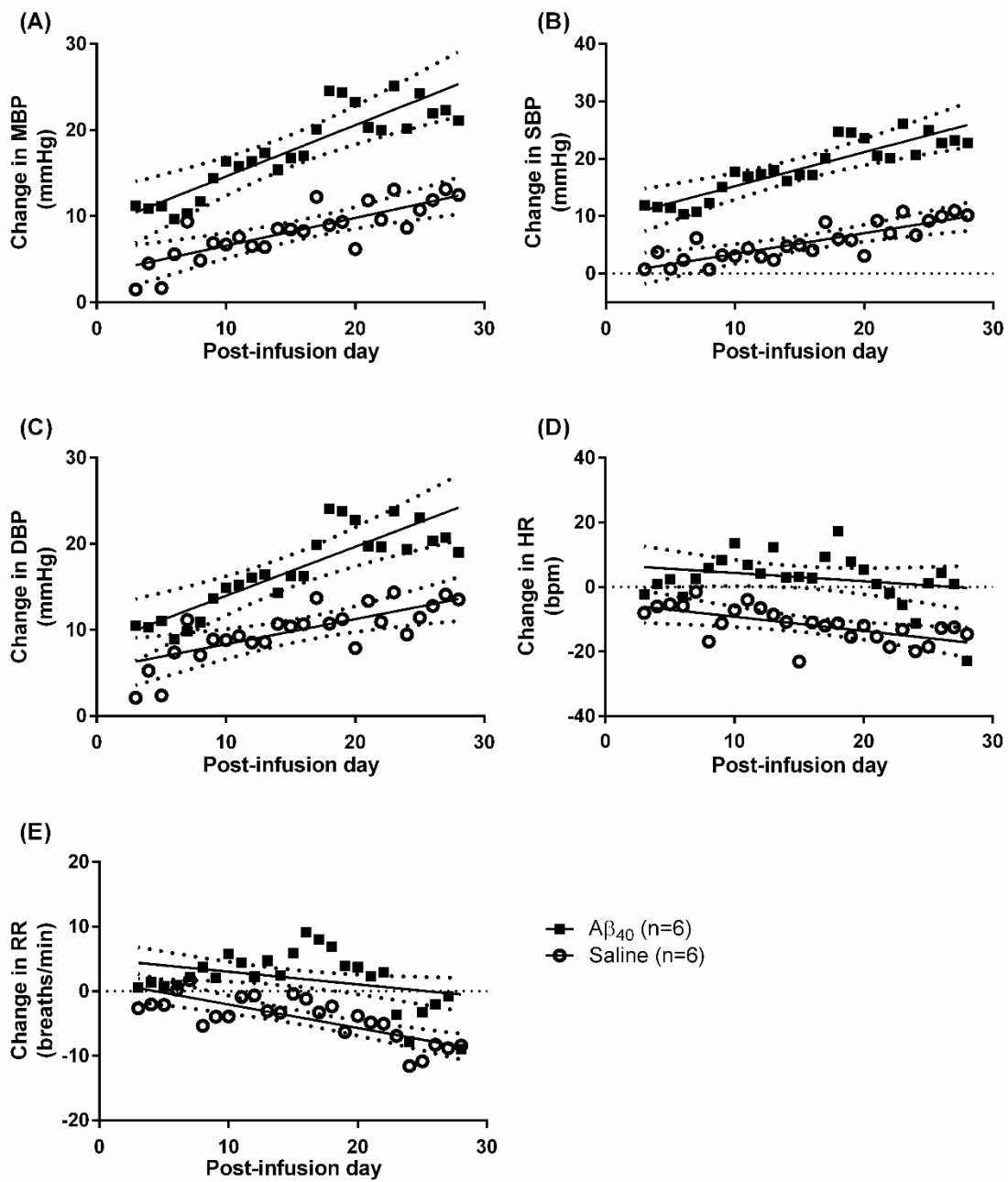
Figure 5 Change in BP, HR and RR in Low-Salt DAHL/SS
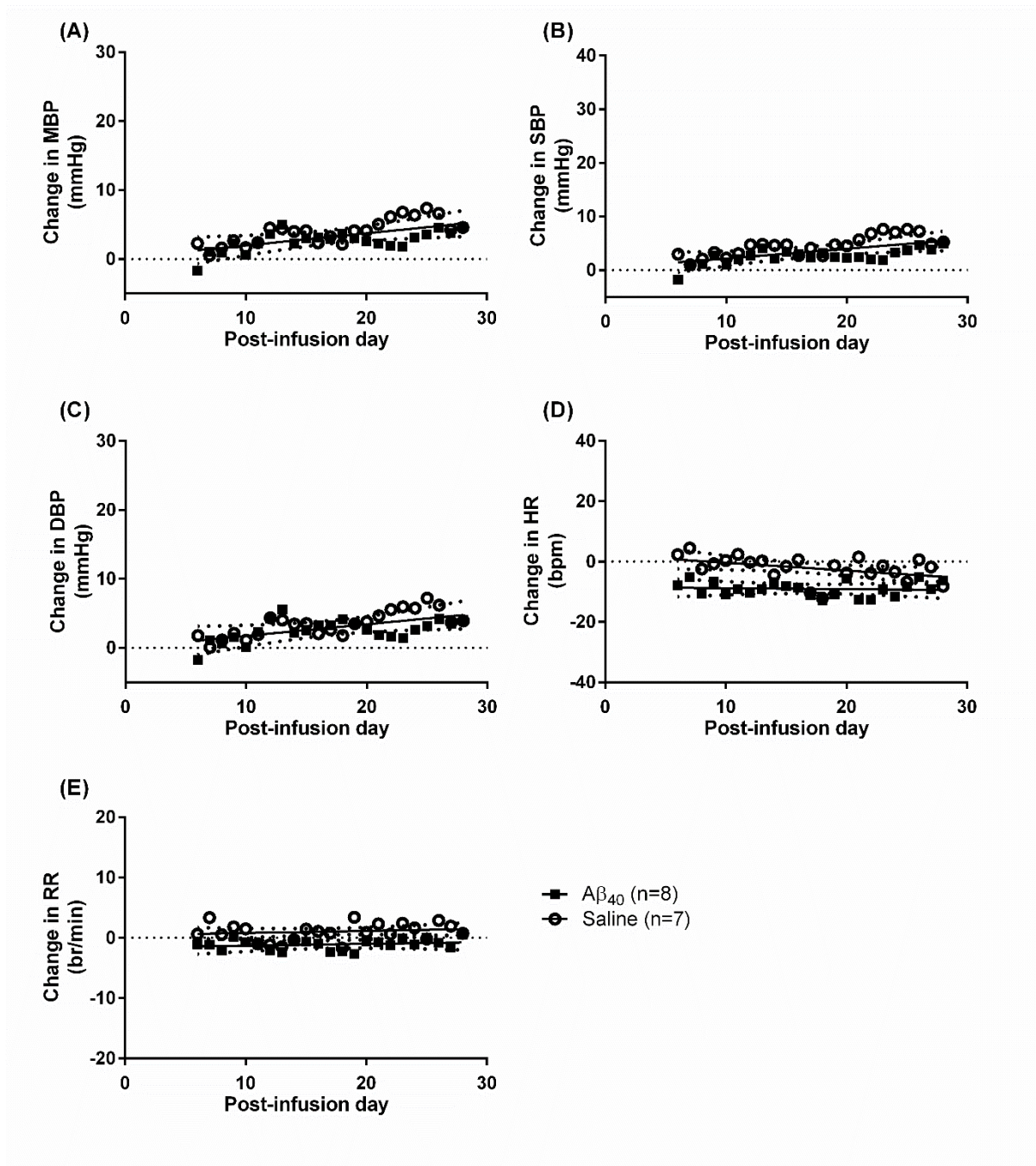
Figure 6 Change in HRV, SBPV and BRG in High-Salt DAHL/SS

Saline (n=3)   ■ Aβ$_{40}$ (n=5)
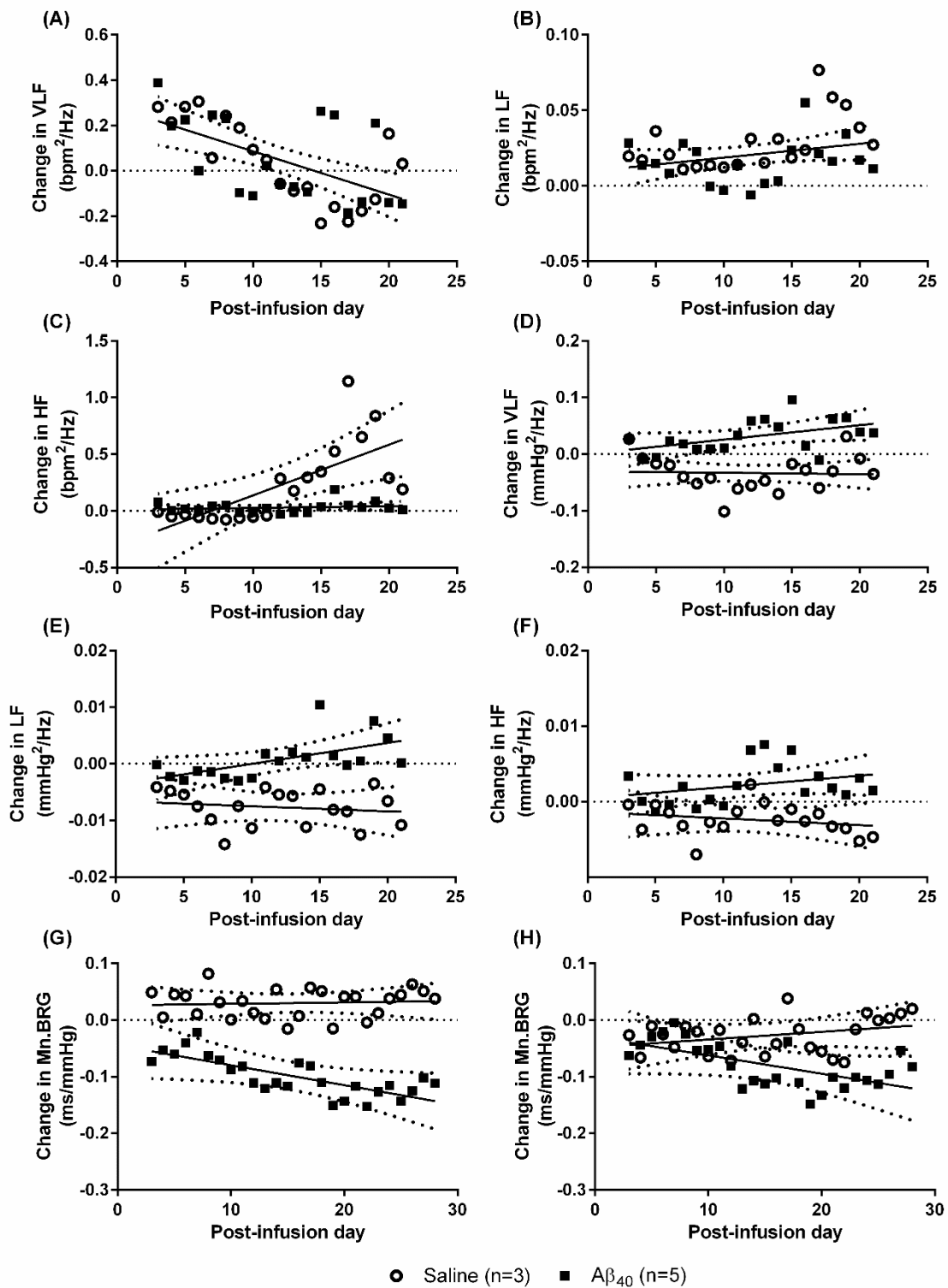
Supplementary Figure Legends

Supplementary Figure 1

Change in BP, HR and RR in high-salt DAHL/SS relative to baseline (day -7 to 0) after either Aβ (n=6) or saline (n=6) infusion (post-infusion data from day 3 to 28). Each data point represents the individual mean value over a given 24-h period, adjusted to the baseline mean value for the same individual.

Supplementary Figure 2

Change in BP, HR and RR in low-salt DAHL/SS relative to baseline (day -7 to 0) after either Aβ (n=8) or saline (n=7) infusion (post-infusion data from day 3 to 28). Linked scatter plots represent data points for the individual mean value on a given 24-h period, adjusted to the baseline mean value for the same individual.

Supplementary Figure 3

Change in HRV, SBPV and mean BRG in high-salt DAHL/SS relative to baseline (day -7 to 0) after Aβ (n=5) or saline (n=3) infusion (post-infusion data from day 3 to 28). Linked scatter plots represent data points for the individual mean value on a given 24h period, adjusted to the baseline mean value for the same individual.

Supplementary Figure 4

MBP in high- and low-salt DAHL/SS following Aβ-/saline-infusion. A paired t-test was used to compare MBP in the final week following infusion (day 22-28 inclusive) relative to pre-infusion baseline. MBP in (A) low-salt DAHL/SS increased after Aβ infusion (day 22-28 vs. baseline) by 3 ± 3 mmHg (t (7) = 2.948, p = 0.022), but did not change significantly after (B) saline infusion. MBP in the (C) high-salt DAHL/SS increased by 21 ± 11 mmHg (mean ± SD) in the Aβ group (t (5) = 4.726, p = 0.005), whereas MBP in the (D) saline group increased by 11 ± 8 mmHg (t (5) = 3.635, p = 0.015).

Supplementary Figure 5

$A\beta_{40}$, ET-1, ECE-1, ECE-2 levels and ACE activity in high- and low-salt DAHL/SS after Aβ or saline infusion. No significant difference was found in $A\beta_{40}$ level in the high- or low- salt DAHL/SS after 4 weeks' Aβ-

28

infusion in (A) brain tissue homogenates (mean + SD). In (B) plasma samples, Aβ_{40} levels were lower than in brain tissue homogenates and several cases fell below the detection limit of the assay; no significant difference was found in the Aβ_{40}- compared with saline-infused high- or low-salt DAHL/SS (median + IQR shown as data skewed to left). No significant differences were found in the levels of EDN1, ECE-1 or ECE-2 in brain tissue homogenates. Mean + SD of total (C) EDN1 (pg/ml) (D) ECE-1+ECE-1sv (pg/ml) (E) ECE-2 (ng/ml) are shown, presented as mean results from left and right-brain homogenates combined. ACE activity in high and low salt DAHL/SS in (F) brain tissue homogenates; (G) plasma. No significant difference was found between Aβ-infused brain tissue homogenates with respect to ACE activity.

Supplementary Figure 6

Example power spectral components and time series data for variability and baroreflex sensitivity analyses. HR and SBP waveforms were analysed by use of Spike2 with the HRV1.s2s script, with a (A) 60-s epoch duration shown. A SPBV power spectrum example (B) is shown for the 60-s period above, with the vertical lines to indicate the low and high edges of the frequency bands analysed (VLF 0-0.26 Hz; LF 0.26-0.76 Hz; HF 0.76-3.3 Hz). An example results table (C) is also shown. Baroreflex sensitivity was analysed by use of Spike2 software running the sBRG.s2s script, reflecting spontaneous fluctuations in BP and pulse interval. (D) a smoothed BP and pulse interval trace is generated, and ramps are marked during which BP rises or falls consistently over several heartbeats. (E) Example plot of a positive ramp (R+), and (F) of a negative ramp (R-) show the blood pressure vs. changes in pulse interval after 3, 4, and 5 heartbeats. The baroreceptor reflex sensitivity was estimated from the linear best fit of this correlation. The threshold for the mean r^2 statistic for each plot was set to 0.7 and ramps with an $r^2<0.7$ were rejected (yellow).
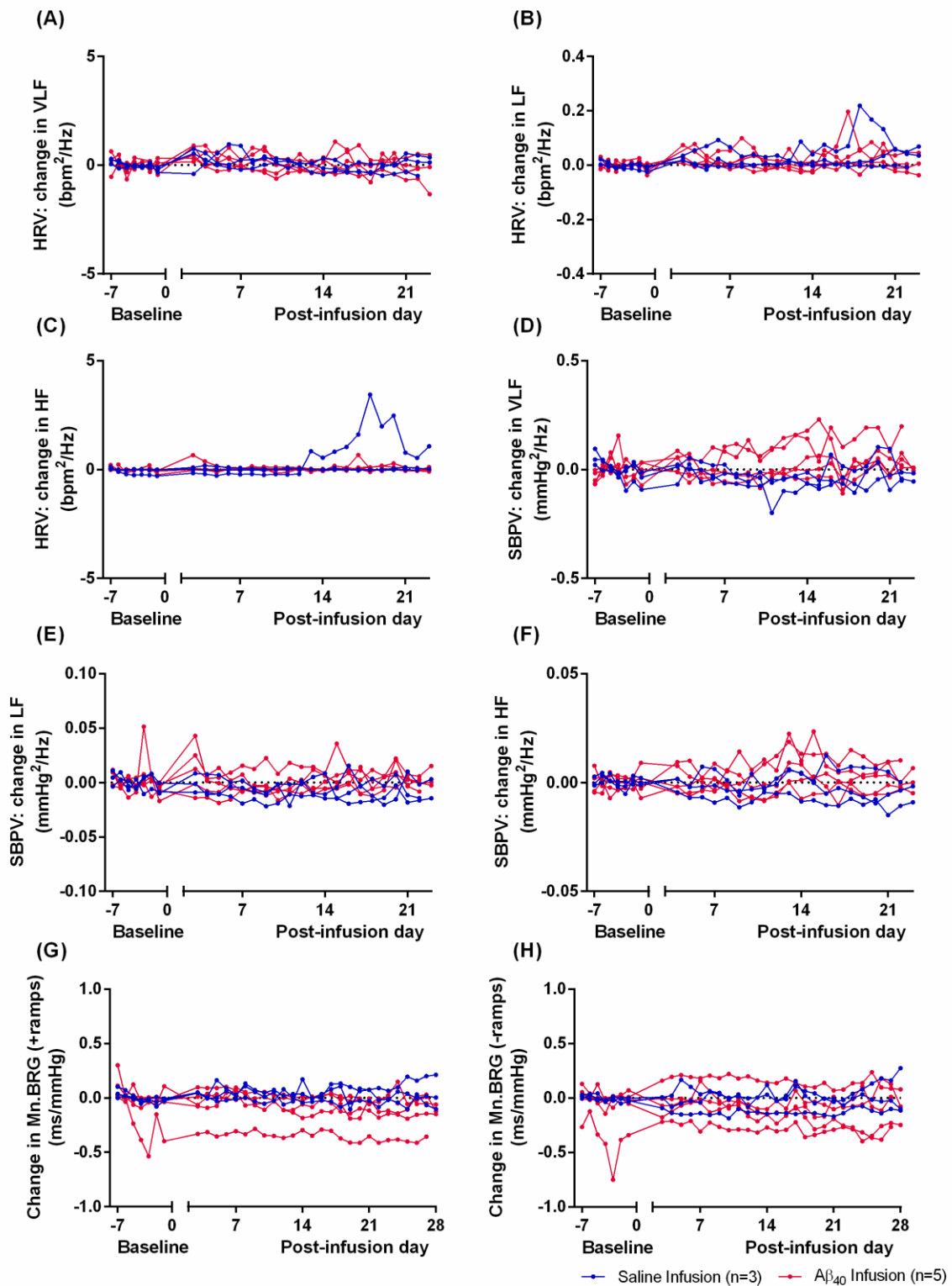
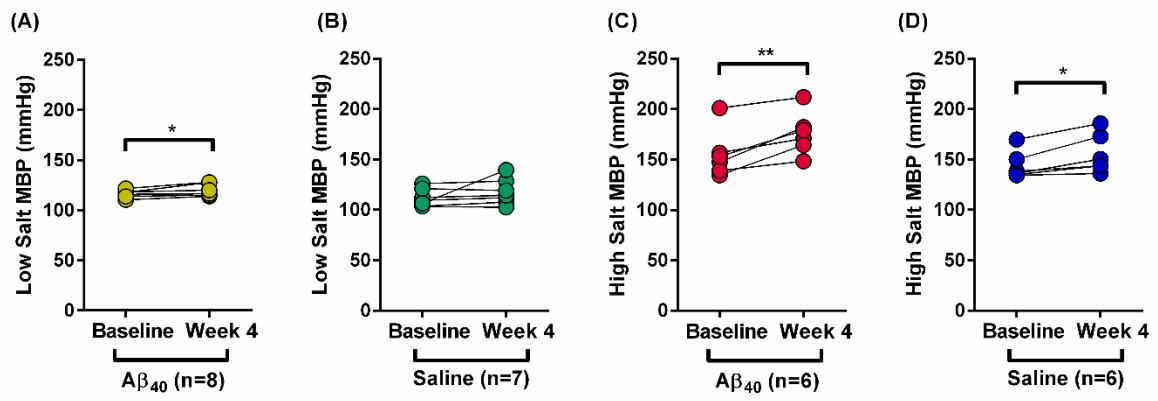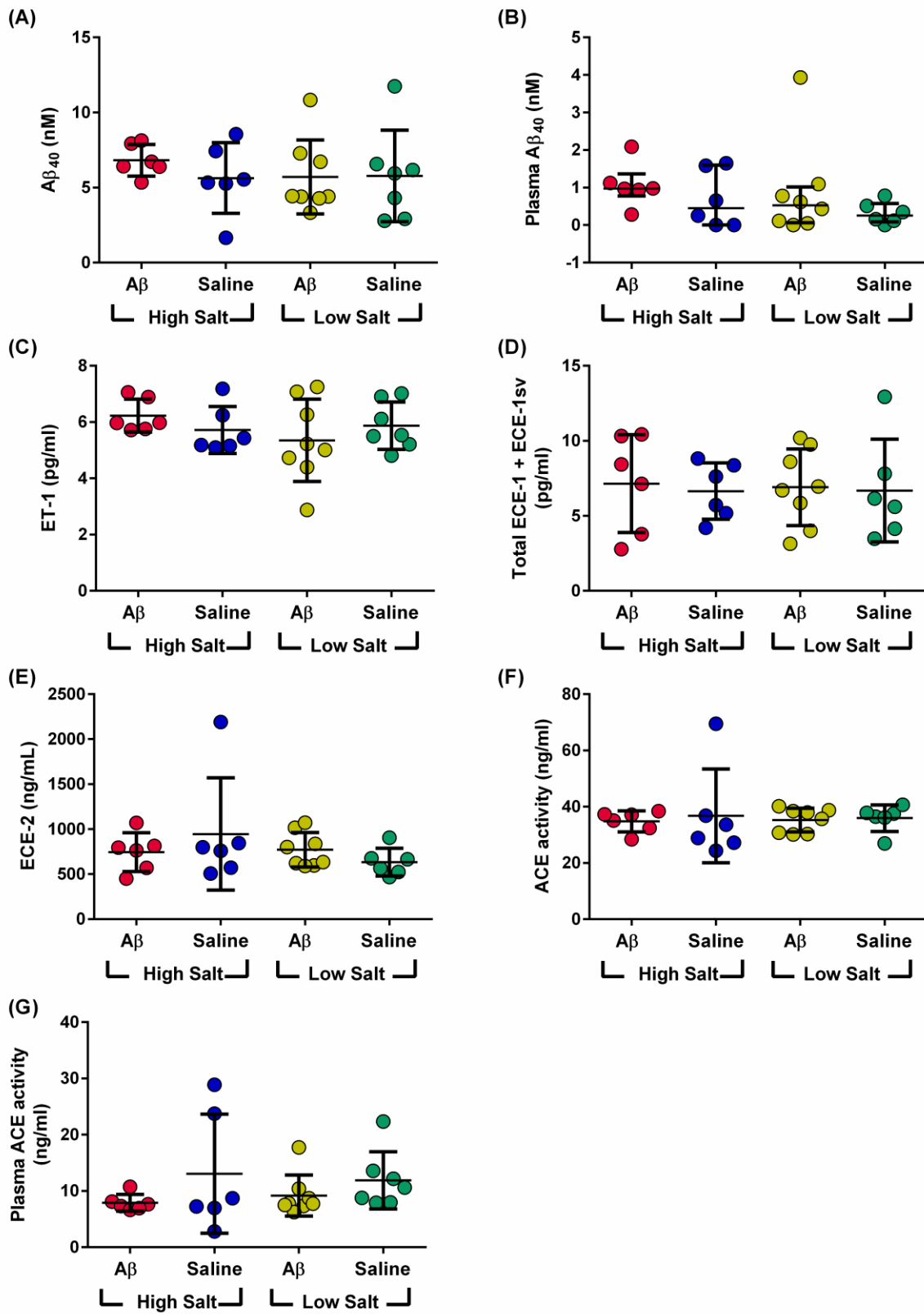# Supplementary Figures

Supplementary Figure 1
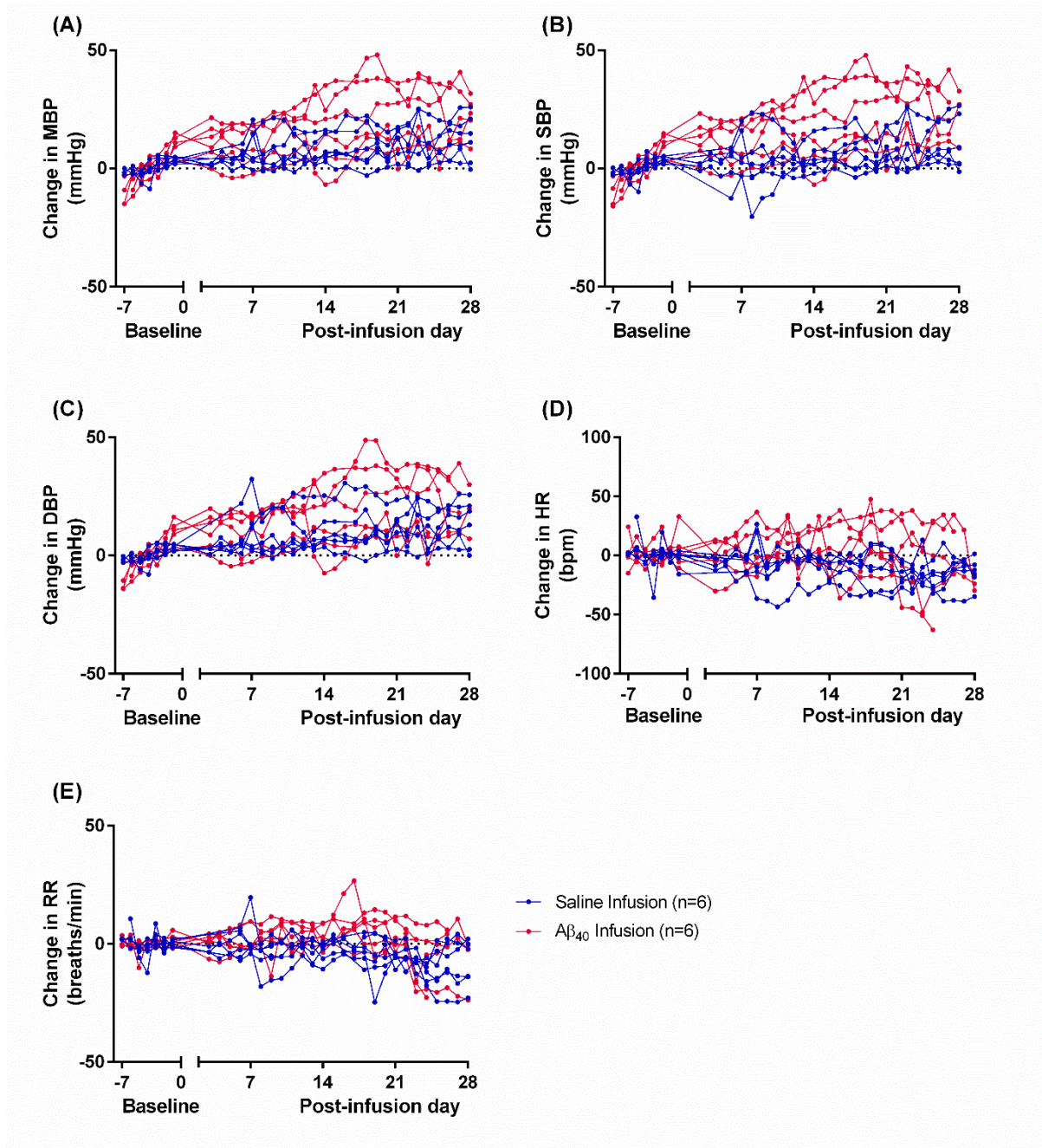
Supplementary Figure 2
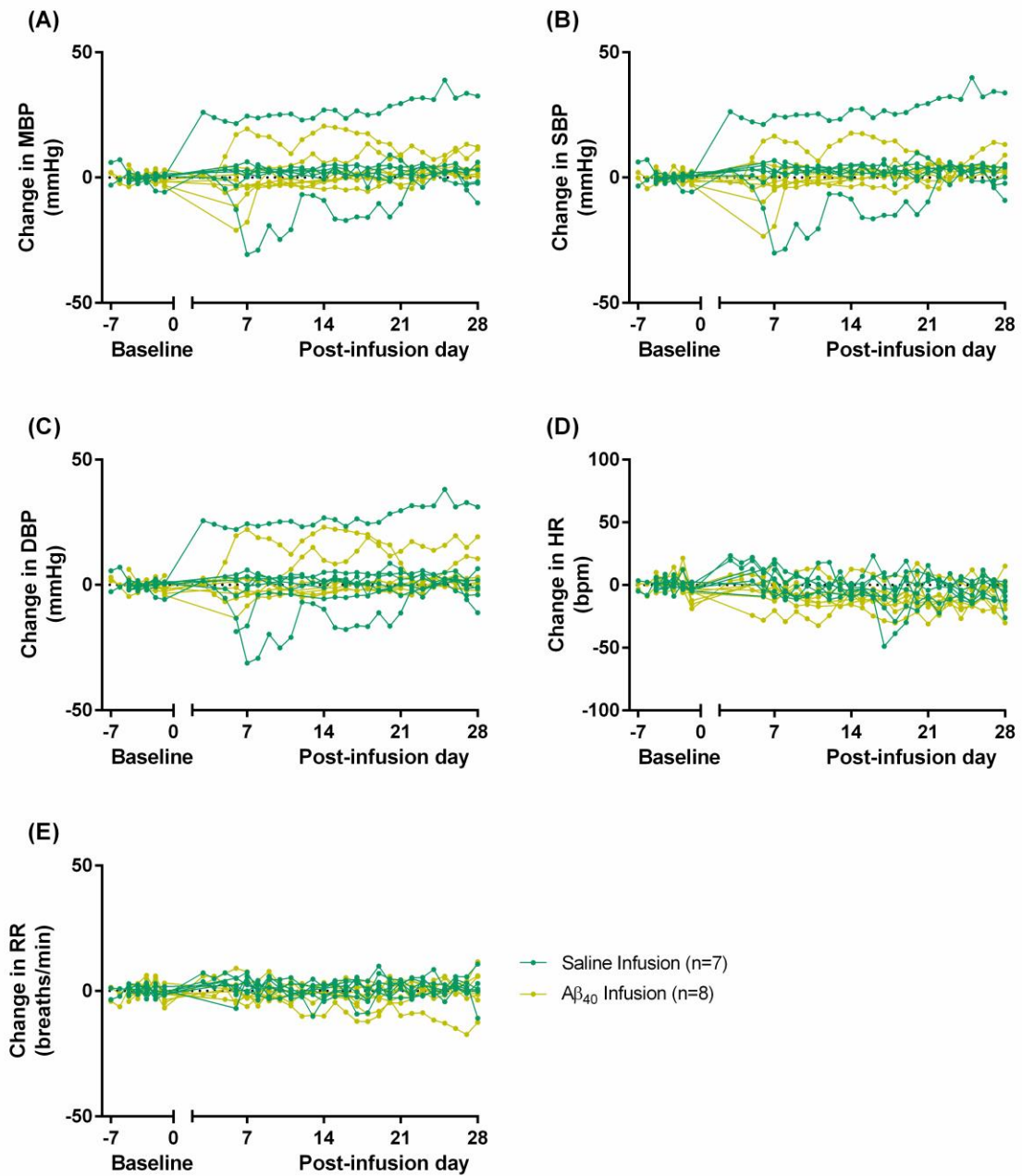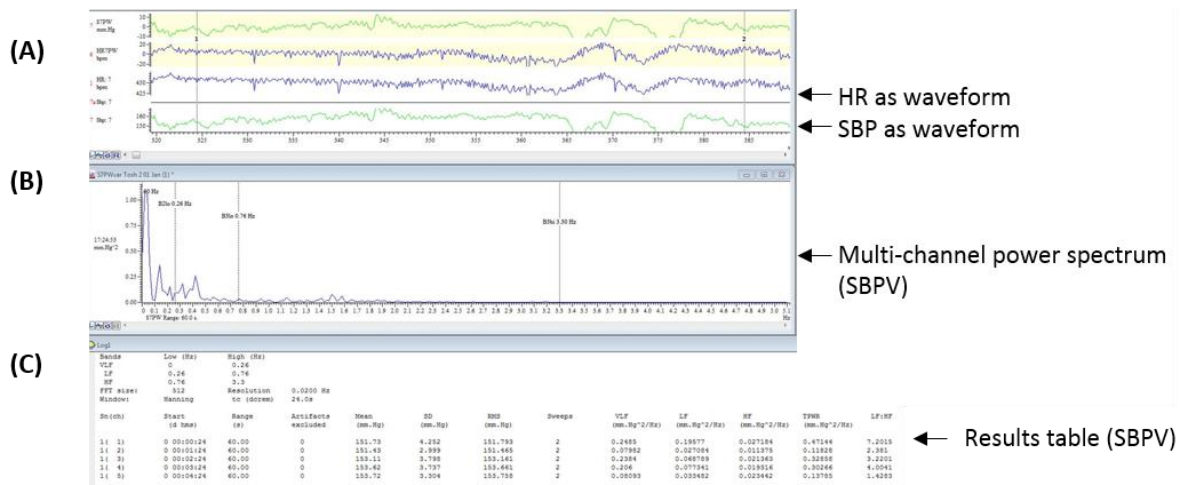
Supplementary Figure 3

Supplementary Figure 4

Supplementary Figure 5

Supplementary Figure 6

HRV and SBPV power spectra
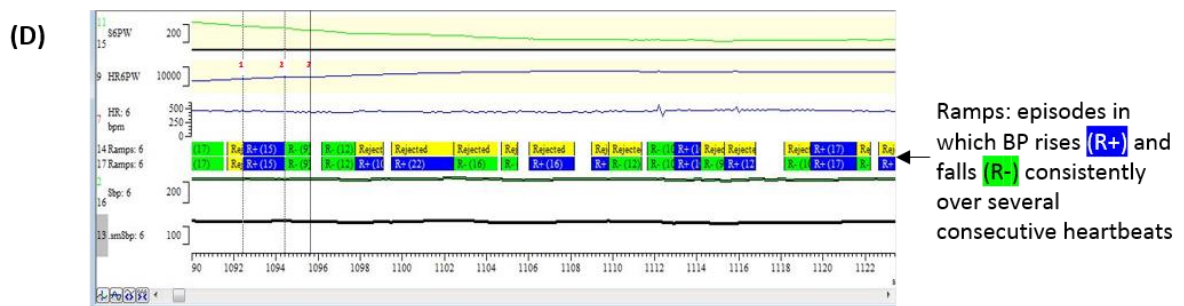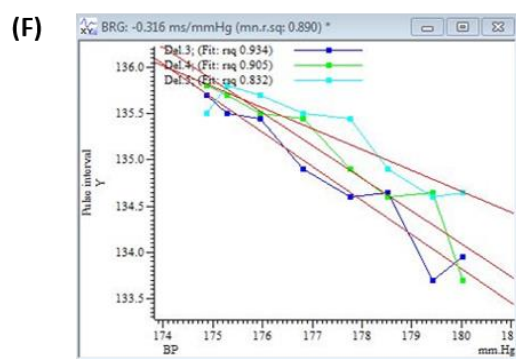

(A) ← HR as waveform
← SBP as waveform

(B) ← Multi-channel power spectrum (SBPV)

(C) ← Results table (SBPV)

Baroreflex sensitivity

(D) ← Ramps: episodes in which BP rises (R+) and falls (R-) consistently over several consecutive heartbeats

(E)

(F)
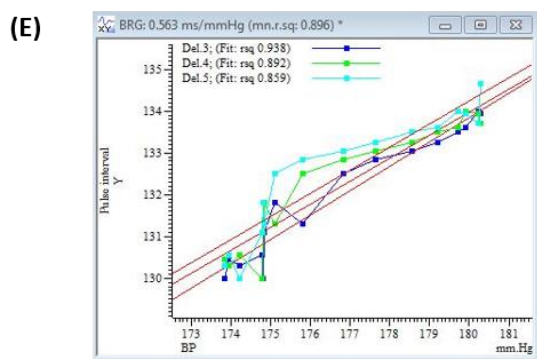
Positive ramp example
- Onset (s): 1089.35
- Duration (s): 2.18
- Beats (n): 16
- BP change (mmHg): 6.448
- Mean.sBRG (ms/mmHg): 0.563
- mean r^2 = 0.896

Negative ramp example
- Onset (s): 1094.41
- Duration (s): 1.97
- Beats (n): 8
- BP change (mmHg): -5.115
- Mean.sBRG (ms/mmHg): -0.316
- mean r^2 = 0.890